Current Applied Science and Technology Vol. 23 No. 4 (July-August 2023)

Research article

A Green Product Using Selective Compound for Susceptible Assessment of Copper in Blood Serum

Hussain Kirem[1] and Naser Abdulhasan Naser[2]*

[1]*College of Pharmacy, The Islamic University, Najaf 54001, Iraq*
[2]*Department of Chemistry, Faculty of Science, University of Kufa, P.O. Box (21), Najaf Governorate, Iraq*

Received: 25 July 2022, Revised: 16 September 2022, Accepted: 20 December 2022

DOI: 10.55003/cast.2022.04.23.008

Abstract

A highly reliable approach for assessment of copper(II) in blood serum samples using an organic molecule 4-(3-hydroxyphenylazo)resorcinol, 4-HAR was developed. The paper presents the synthesis of 4-HAR, which serves as probe for definite species. 4-HAR was characterized with the FT-IR, UV-visible, ^{1}H-NMR, ^{13}C-NMR and mass analysis, thermal TG and DSC techniques. After examining its interactions with more than twenty-five metal ions, it was found that 4-HAR showed reaction only with copper(II), giving a distinct green color at λmax 603 nm. Experimental conditions for the reaction of 4-HAR with copper(II) were optimized. A calibration curve was created and the exhibition range of concentration obeyed Beer's Law from 0.30 to 16 $\mu g.mL^{-1}$ with correlation coefficient of r = 0.9986, and value of the molar absorption coefficient, ε, being 3314 $L.mol^{-1}.cm^{-1}$. The analytical method was used to determine copper(II) levels in several blood serum samples. The amounts of copper(II) found in the sera samples were compared with flame atomic absorption spectrometry technique, and the results were found to be highly reliable. Based on validation, the new approach can be utilized for assurance quality purposes with a high degree of confidence.

Keywords

blood serum;
copper(II);
assessment;
resorcinol;
solvatochromism;
spectrophotometry

1. Introduction

Transitional elements are necessary in most biological and environmental systems [1, 2]. However, their enormous significance results either from their critical significance in biological pathways or because of their dangerous nature. One of these transition metals is copper. It is the third most abundant trace element in the human body, with low concentrations found in a wide range of cells and tissues [3, 4]. One of the most crucial components in the biology of living things is copper. It is

*Corresponding author: Tel.: (+96)7802424994
E-mail: nasir.almutawiri@uokufa.edu.iq

a necessary nutrient that is required for many biomedical processes, along with the production of proteins and the expression of genes [5]. Copper is a vital micromineral because a lack of it in the body can result in anemia, neutropenia, and bone abnormalities [5, 6]. Even so, too much copper consumption, on the other hand, can cause gastrointestinal problems, liver and kidney damage, as well as neuropathological diseases. By the way, in today's societies, industrial development in the areas of electronics, thermal conductors, and metal alloys have led to increased consumption of copper, and environmental and biological contamination has followed. [7]. The World Health Organization imposed a limit on the amount of copper that can be present in drinking water at 2.0 ppm (30 nM) [8]. As a result, having powerful analytical tools for measuring copper levels in food and drink samples is critical, and thus research involving the quantitative analysis of copper is highly valued. There are numerous analytical methods for determining the levels of copper (II), atomic absorption spectrometry [9, 10], mass spectrometry using inductively coupled plasma [11, 12], electroanalysis techniques [13, 14], x-ray fluorescence [15], surface plasmon resonance (SPR) spectroscopy [16], and colorimetry [17]. Despite the fact that these methods can yield extremely sensitive and selective results, they have the disadvantages of being difficult to execute and requiring time-consuming procedures [18]. As a result, simple spectrophotometric methods are preferred and are seen as an alternative to methods requiring more complex instrumentation because they are less expensive and labor-intensive. Various spectrometric techniques using different reagents such as Zincon [19], PAR [20], 4-Br-BTAP [21], dPKBH [22], nitroso-R salt [23], cuprizone [24], PAN [25], naphthazarin [26] and 2-APT and 3-APT [27] have been utilized for Cu(II).

In the present work, a sensitive organic reagent, 4-(3-hydroxyphenylazo)resorcinol, or 4-HAR, has been synthesized. It contained a suitable functional group that permits the reaction with copper under optimum conditions to give a corresponding analytical signal. 4-HAR selectively develops a green product with Cu(II), which facilitates its use in an analytical method for the determination of copper in blood serum.

2. Materials and Methods

2.1 Instruments

The UV-visible spectra were recorded using quartz cells of 1 on an ultraviolet–visible spectrophotometer (T80- PG Instruments Ltd., UK). FT-IR spectrophotometer was used to measure the spectra (Prestige-21FT-IR, Shimadzu, Japan). Melting points were measured via a melting point apparatus (SMP30 Stuart, UK) and were not amended. The measurements of pH were achieved using a calibrated pH meter (WTW 340i, Germany. Using Stapt-1000 Linseis). Thermal analysis was measured by differential calorimetry and thermogravimetric scanning. Thermal testing of the experiment compound and its raw materials were performed in a continuous pure nitrogen environment (flow rate of 50 mL/min). The device was calibrated with indium. Samples were collected in unsealed aluminum vats and probed at a heating rate of 10°C/min in a platinum crucible from 30°C to 500°C. The ^{1}H-NMR spectrum was measured at 400 MHz in DMSO as a solvent with a spectrophotometer (Bruker DPX 400 NMR). Chemical shifts were documented in parts per million using TMS as an internal standard.

2.2 Materials

All solutions of chemicals used were prepared in water and were all of the analytical reagent grade. Resorcinol and 3-aminophenol were supplied by Sigma Aldrich. Solvents like chloroform, ethanol, diethyl ether, benzene, ethyl acetate, methanol were supplied by BDH, RDH, Merck, and GCC

provided acetic acid, n-butanol, propanol, toluene, DMSO, acetonitrile, and THF. Solvents were employed with no modifications. Silver nitrate, sodium nitrite and sodium hydroxide were provided by Fluka.

2.3 Synthesis of 4(3-hydroxyphenylazo) resorcinol (4-HAR) [28]

A 1.0913g (0.01 mol) of 3-aminophenol was dissolved in a solution of 5 mL concentrated hydrochloric acid and 40 mL distilled water. In an ice bath, the solution was cooled to 0 to 5°C, and a sodium nitrite solution, which had been pre-made by combining 5 mL of distilled water with 0.60g (0.01mol) of sodium nitrite, was gradually added. The diazotization process was allowed to continue for 1h. A 1.1g (0.01 mol) of resorcinol in 40 mL of distilled water was added as a coupling component to the diazonium salt slowly with good stirring at pH less than 7. The product was left for 24 h to complete the settling process. The product yield was 60% after the red precipitate was filtered, recrystallized with absolute methanol, and dried. The reaction is shown in Figure 1.

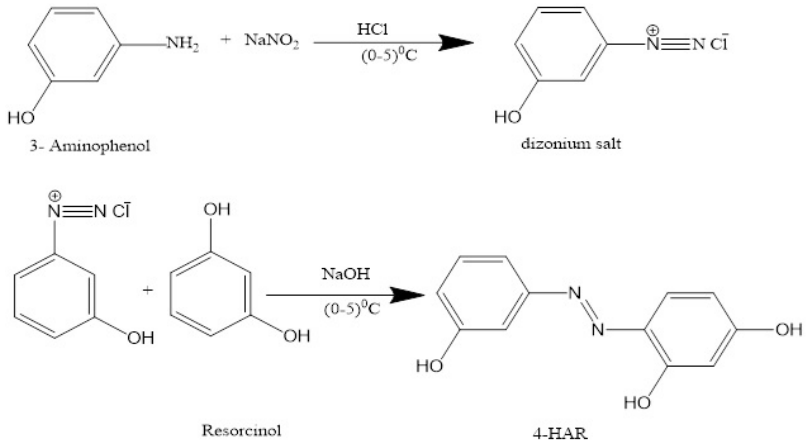

Figure 1. Synthetic route of 4-HAR

2.4 Preparation of solutions for the analytical application of 4-HAR

2.4.1 4-HAR stock solution, (0.0010 M)

Working solutions were prepared by dissolving 0.0058 g in 25 mL absolute methanol to achieve the desired concentration.

2.4.2 Copper (II) solution, 0.045 M

The solution was prepared by adding 0.5618g of copper sulphate pentahydrate to distilled water, and the volume was made up to 50 mL in a volumetric flask.

2.4.3 Sodium hydroxide solution, 1.0 M

A 2.0g of sodium hydroxide was prepared in distilled water, and volume was made to 50 mL in a volumetric flask.

2.4.4 Spectrophotometric assay for Cu(II)

A number of 10 mL standard volumetric flasks were prepared. Following the addition of 2.0 mL of reagent solution at 50°C, various volumes of Cu(II) stock solution were transferred to achieve a concentration range of 0.3-16 $\mu g.mL^{-1}$ for Cu(II). After optimizing the pH of the medium (pH =8.0) and the reaction time, the contents of each volumetric flask were thoroughly mixed (20 min). At 603 nm, the absorbances of the Cu(II) complex were measured in comparison to the similarly prepared reagent without the metal ion.

2.4.5 Procedure for the determination of Cu (II) in blood serum of participants

The participants were individuals who had in some form contributed to the development on the Cu(II) spectrophotometric assay. For the purposes of the current study, human biological samples such as blood and serum were needed to test the capability of Cu(II) analysis technique. Human blood and serum were chosen as there are easy samples to collect from patients. Patient samples were collected by AL-Sadder Hospital in Najaf governorate These samples were collected as de-identified pathologic discard as whole blood and serum samples.

1) Protein precipitation

There are many different procedures for this purpose. A protein precipitation method using organic solvents (absolute ethanol) was adopted in the current study.

2) Spectrophotometric procedure

To prepare the sample for analysis, 1 ml of serum was poured into a test tube and 2 mL of ethanol was added as deproteinizing agent. The contents were then centrifuged at 4000 $turns.min^{-1}$. After the deproteinization process, the sediment was filtered off and discarded. To the filtrate, sodium fluoride was added to cover up the iron in the sample [29]. After that, 1 mL was taken from the supernatant and the copper(II) present in serum was estimated by the recommended spectrophotometric method at 603 nm.

3. Results and Discussion

3.1 Physical and chemical features of 4-HAR

Both thin-layer chromatography (by toluene: methanol at a ratio of 2:3) and melting point were used to assess the purity of the organic reagent. The reagent was a dark red powder that was insoluble in water, but soluble in methanol, ethanol, acetone, dimethylformamide, and dimethyl sulfoxide. The reagent solution had a yellow color at a pH less than 5, although in the alkaline medium it had a deep orange color.

4-HAR melted at 217°C. Figures 2, 3 and 4 show the FTIR spectra of 3-aminophenol, resorcinol, and 4-HAR, respectively. These compounds share among them the presence of -C=C-, Ar-H and C-N [30]. FTIR spectroscopy was here utilized to confirm the formation of 4-HAR through the appearance and disappearance of important functional group bands. Figure 2 is characterized by the appearance of two sharp bands at 3350 and 3290 cm^{-1} for a primary aromatic amine while the band at 3257 cm^{-1} belongs to the hydroxyl group of resorcinol, as seen in Figure 3. In the case of 4-HAR, Figure 4 shows the disappearance of the two bands, and the appearance of a

broad band at 3257 cm^{-1} belonging to the resorcinol's hydroxyl group as well as to the new band at 1458 cm^{-1} belonging to the –N=N– group, which emphasize the formation of 4-HAR [31]. Intramolecular hydrogen bonding between the hydroxyl group adjacent to the azo group caused broadening band at 3136 cm^{-1}.

The ^{1}H-NMR spectrum in Figure 5 shows a single peak at δ = 12.8 ppm, which pertains to the OH proton of the resorcinol ring close to the azo group, which was included in an intramolecular hydrogen bond with this group. δ = 10.8 ppm refers to other hydroxyl groups in the resorcinol ring, while the hydroxyl group to other aromatic ring near δ = 9.7-9.9 ppm. As for the peak at δ = 2.5 ppm, it is caused by the solvent DMSO-d6. Signals from δ = 6 to 8.0 ppm belong to protons of the two moieties on either side of the azo group. The appearance of a wide chemical shift at approximately 4 ppm can be attributed to the solvent used, DMSO-d6, which is not 100% pure [32].

Figure 6 illustrates the ^{13}C-NMR spectrum of 4-HAR. Table 1 shows assignment of ^{13}C NMR data for each C-type. Figure 7 shows the MS spectrum of 4-HAR. It is clear in the Figure that the peak belonging to the molecular weight of the prepared reagent is (230.2 m/ z), which represents the peak at the end of the spectrum. The ion fragments at the peaks (109.1, 173.1 m/z) belong to the resorcinol and aromatic rings, respectively. The reagent loses these small particles and they are represented by other unstable peaks in the MS spectrum [33, 34].

In Figure 8, it can be seen that two formulas were proposed for the aryl azo dye found in two tautomeric forms, and it appears that there was no band at the frequency 3500, 1700 cm^{-1} belonging to the secondary amine and carbonyl as shown within the FT-IR spectrum of reagent, so the prepared reagent exists in the enol form with two hydroxyl groups [35, 36].

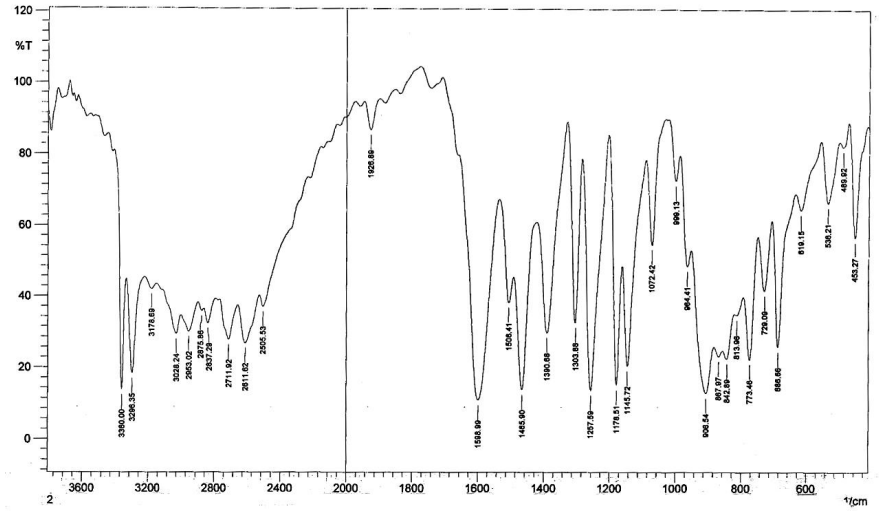

Figure 2. FTIR spectrum for 3-aminophenol

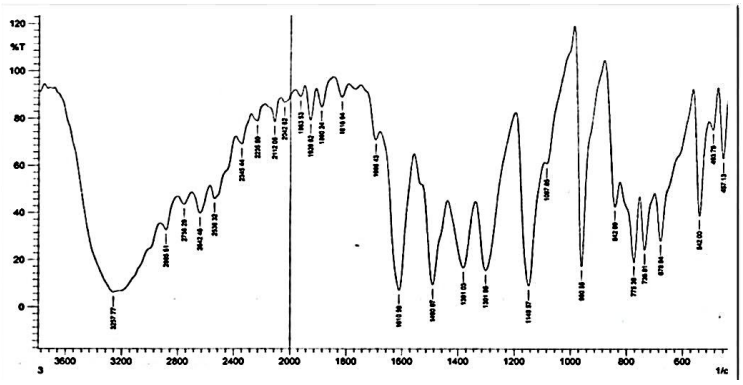

Figure 3. FTIR spectrum for resorcinol

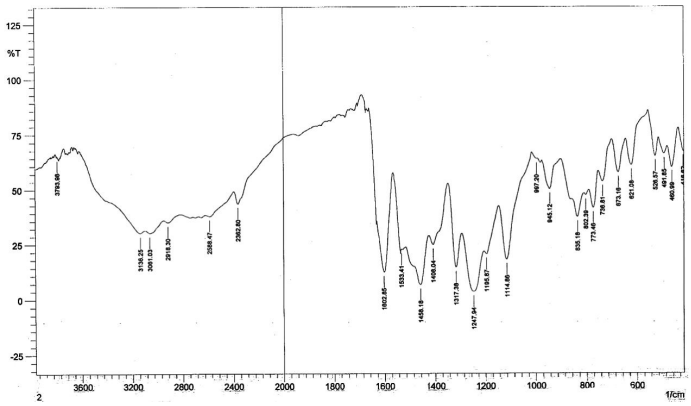

Figure 4. FTIR of 4-HAR

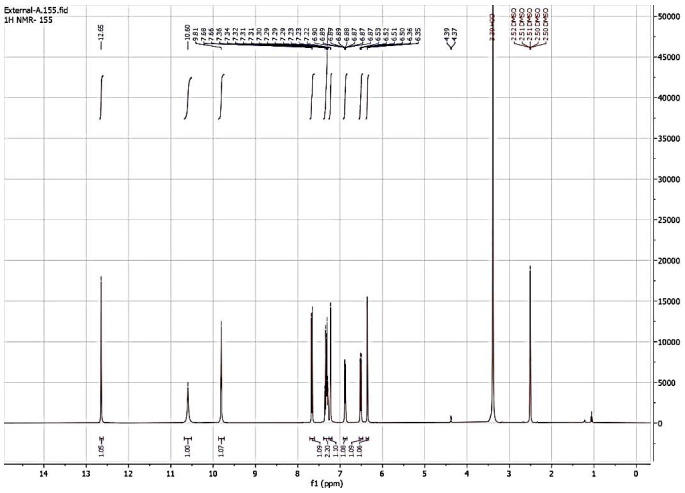

Figure 5. ^{1}H-NMR spectrum of 4-HAR

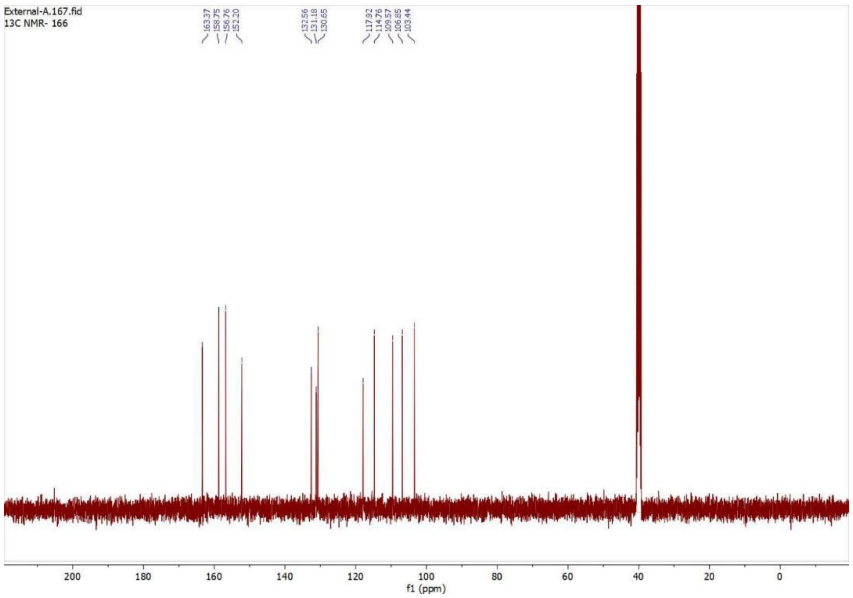

Figure 6. ^{13}C-NMR spectrum of 4-HAR

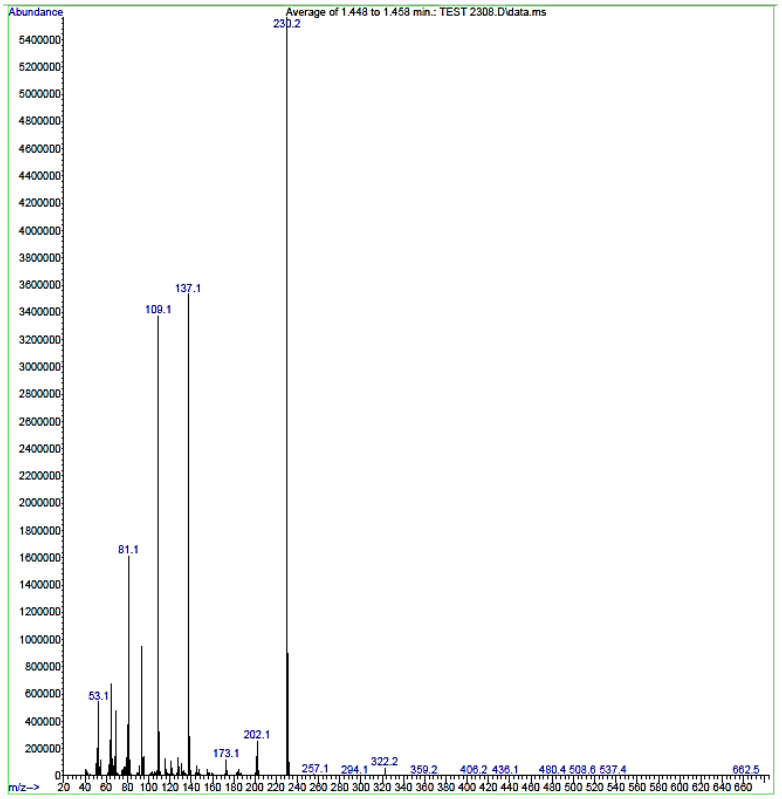

Figure 7. Mass spectrum of 4-HAR

Table 1. ^{13}C NMR data (in DMSO-d6) for the synthesized compound

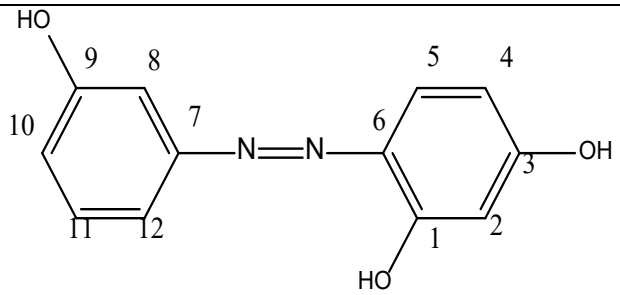

C-Type	C1	C2	C3	C4	C5	C6	C7	C8	C9	C10	C11	C12
^{13}CNMR data & (ppm)	164	131	152	133	114	158	156	118	130	116	113	112

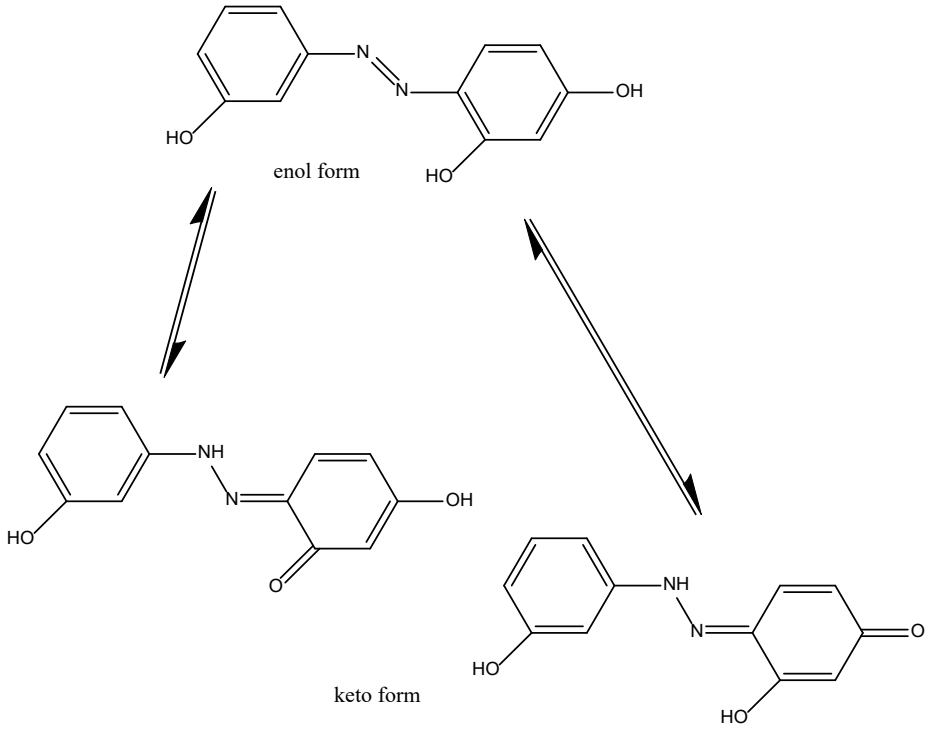

Figure 8. Tautomeric forms of 4-HAR

3.2 Thermal analysis of 4-HAR, thermogravimetric analysis (TG) and differential scanning calorimetry (DSC)

Thermal analysis involves many methods that analyze the properties of a substance based on temperature. Thermal analysis methods, in general, allow pyrolysis, decomposition combustion, thermometry, phase changes, and other properties to be studied on limited sample size and in a highly automated manner [37, 38].

For the TG and DSC thermogram, Figure 9 shows the DSC analysis results. The curve shows two prominent peaks, both of which indicate endothermic. The first peak corresponds to the melting of the compound at 217.30°C, and the second peak is caused by the decomposition of compound at 807.11°C. Figure 10 shows the TG curve and two stages were observed. The first step at 190-220°C with weight loss of 11.739% corresponded to water loss (1.5 molecule) from the surface and pores of the powder compound, and the second step at 400-780°C was attributed to chemical decomposition of the organic compound, with the large loss of mass of 33.704% probably corresponding to the removal of the benzene ring of the compound [39].

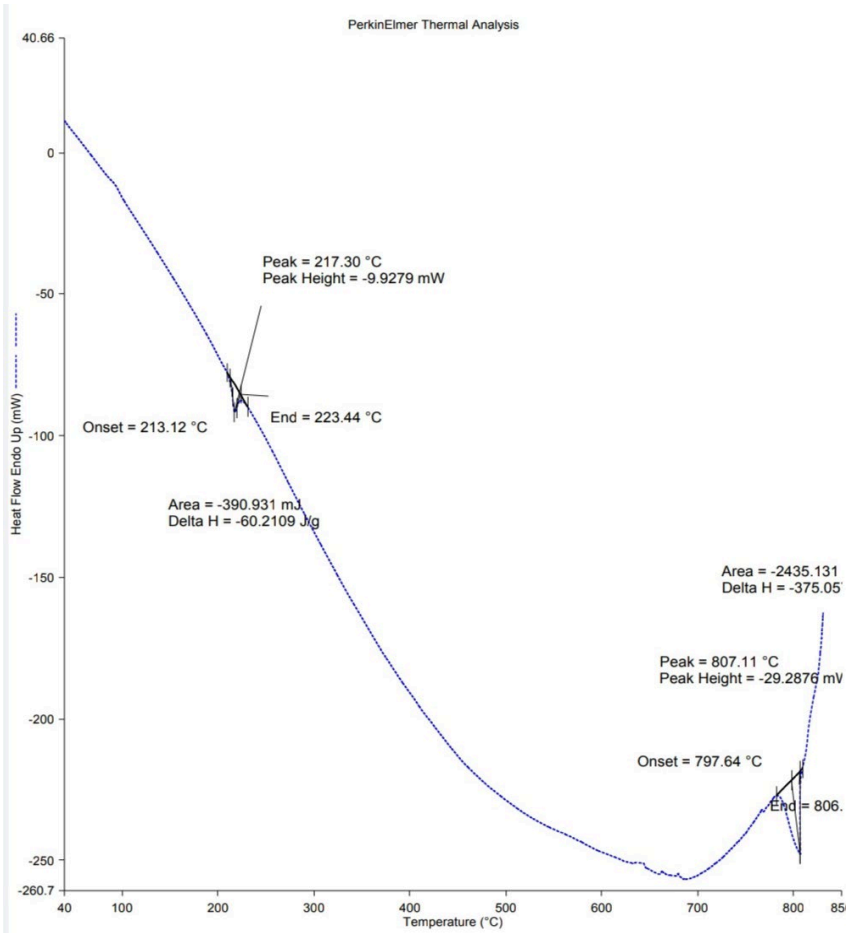

Figure 9. The DSC curve for 4-HAR

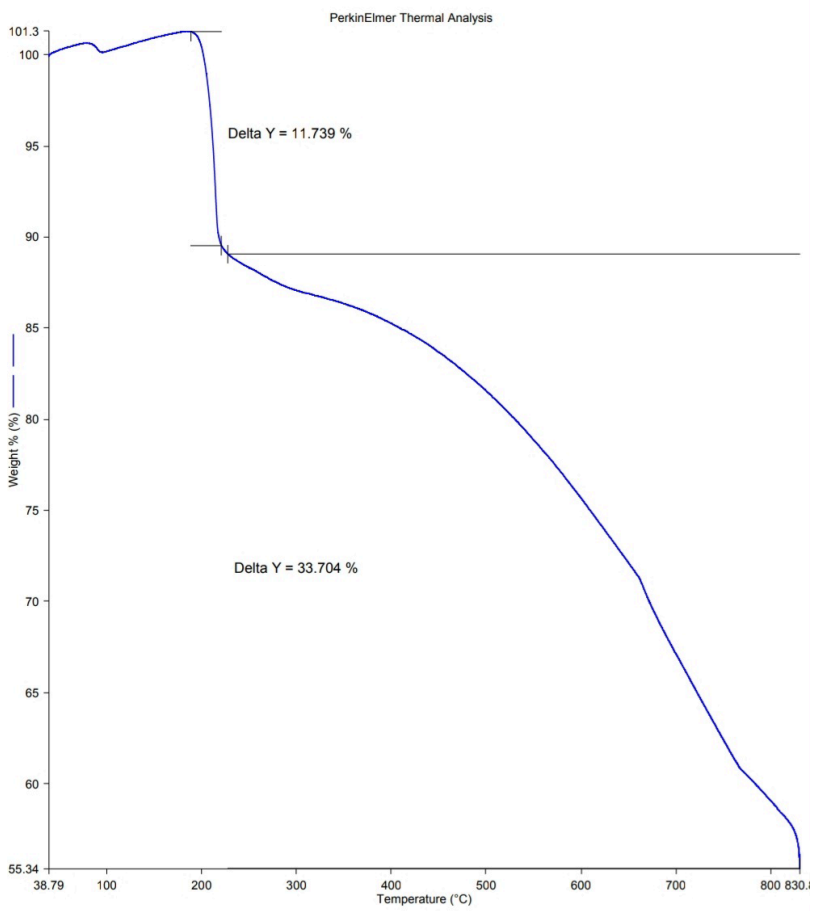

Figure 10. The TG curve for 4-HAR

3.3 Electronic Absorption measurements

The UV-visible spectra of the starting materials, Figures 11 and 12, were measured and showed a maximum absorption which was different from that obtained by 4-HQR. The yellow-colored reagent solution obtained by dissolving 4-HQR in ethanol showed an absorption maximum at 386 nm and was attributed to the -N=N- group, as shown in Figure 13.

Figure 14 shows the effect of pH on a 4-HAR solution within the range from 1.5 to 13 and shows the isobestic point of 4-HAR at 400 nm. Value of pH is 5.6 when the reagent concentration was 2×10^{-4} M that indicates 4-HAR had a slightly acidic nature. Peak at 386 nm showed changes in both positions (bathochromic shift) and intensity within the studied pH range. The 4-HAR solution comprises two acid-base forms, which are: LH_3, LH_2^-, as seen in Figure 15. The LH_3 is the neutral form of 4-HAR, and is of yellow color when pH is varied from low values to 7.5. At pH >8.5, the 4-HAR molecule changes its color into orange as a result of the suggested depiction that shows the molecule bears single negative charge, anionic form LH_2^-, with maximum absorption at wavelength of 445 nm [40, 41].

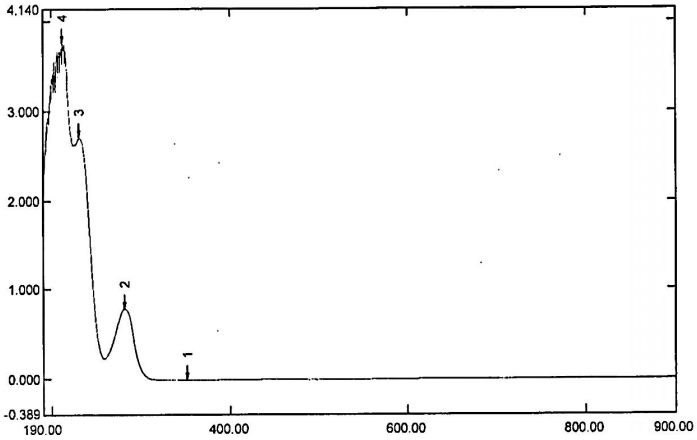

Figure 11. UV-Visible spectrum for 3-aminophenol

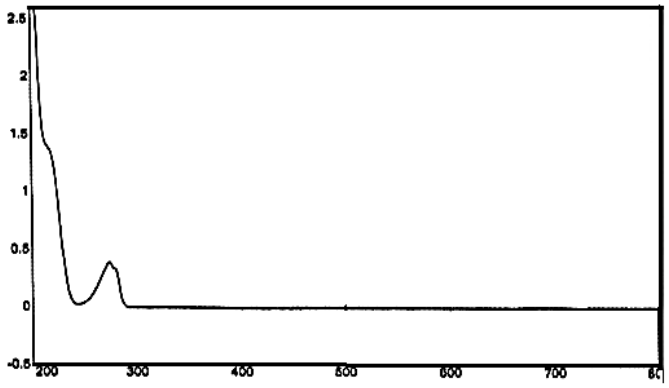

Figure 12. UV-Visible spectrum for resorcinol

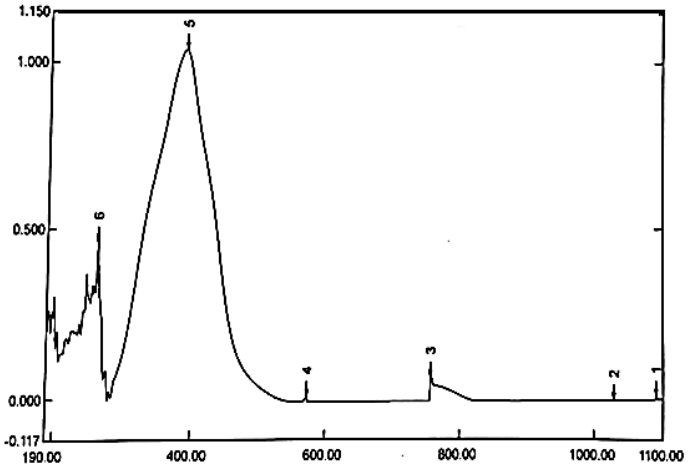

Figure 13. UV-Visible spectrum for 4-HAR

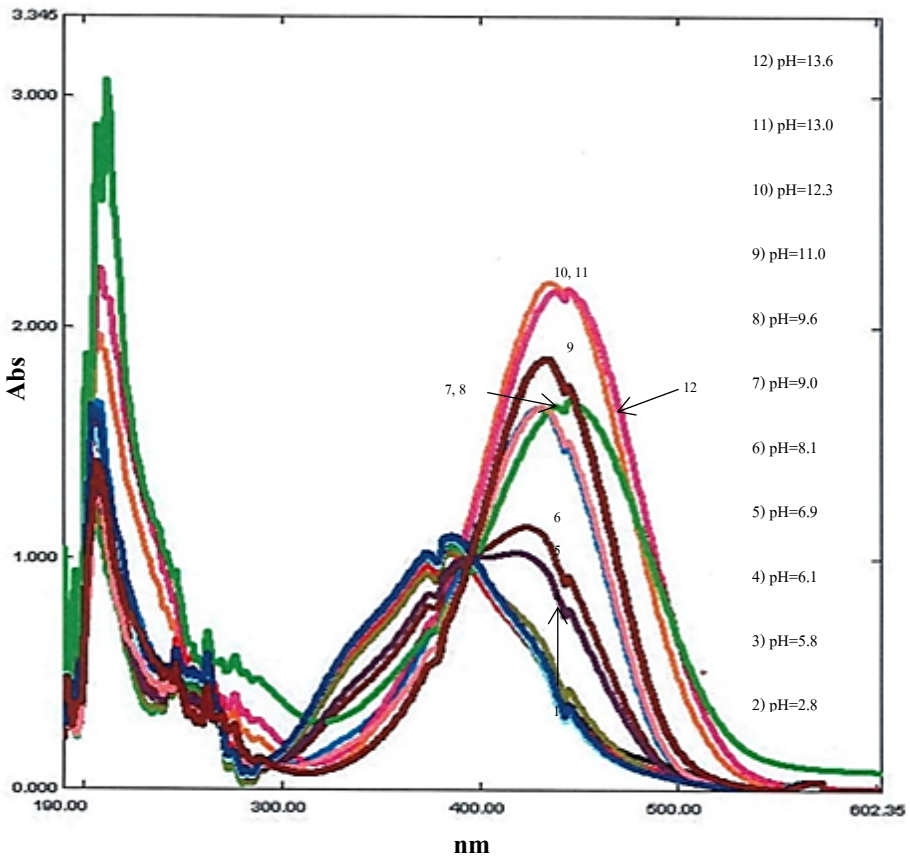

Figure 14. Absorption spectra of 4-HAR reagent at range of pH=1.5-13.6

3.4 Dissociation constant of 4-HAR

Using spectrophotometry, the dissociation constant of 4-HAR was estimated [42, 43]. Absorbance versus pH values were plotted and shown in Figure 16. The pKa value of 4-HAR was found to be 8.8.

3.5 Solvent effect

After being dissolved in a variety of solvents with different polarities, including ethanol, acetic acid, n-propanol, methanol, n-butanol, isopropanol, 1,4-dioxane, ethyl acetate, diethyl ether, ethylene chloride, and DMSO (Figure 17), the azo compound's absorption spectra were examined.

The Kamlet-Taft relationship [44] was used to conduct research on the effects of the investigated solvents. This linear solvation energy relationship (LSER), shown in equation 1, takes into account multiple parameters, including vo, which is the regression value of the solute property, the solvent dipolarity/polarizability π^*, the solvent hydrogen bond acceptor (HBA) basicity β, and the scale of the solvent hydrogen bond donor (HBD) acidity α. The coefficients s, b, and a in the solvatochromic equation represent relative susceptibilities of the absorption frequencies to the specified solvent parameters:

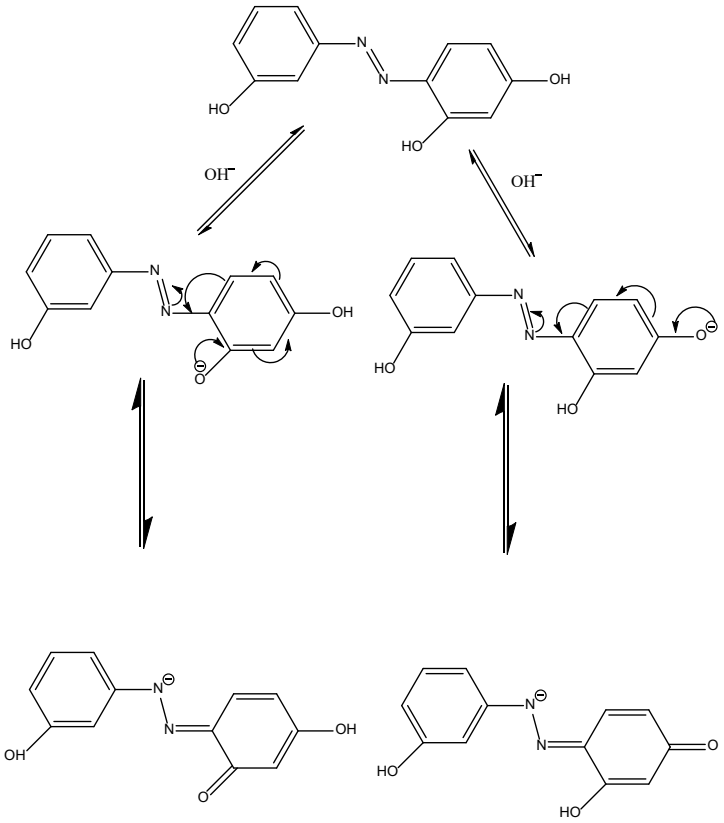

Figure 15. Ionic forms of 4-HAR

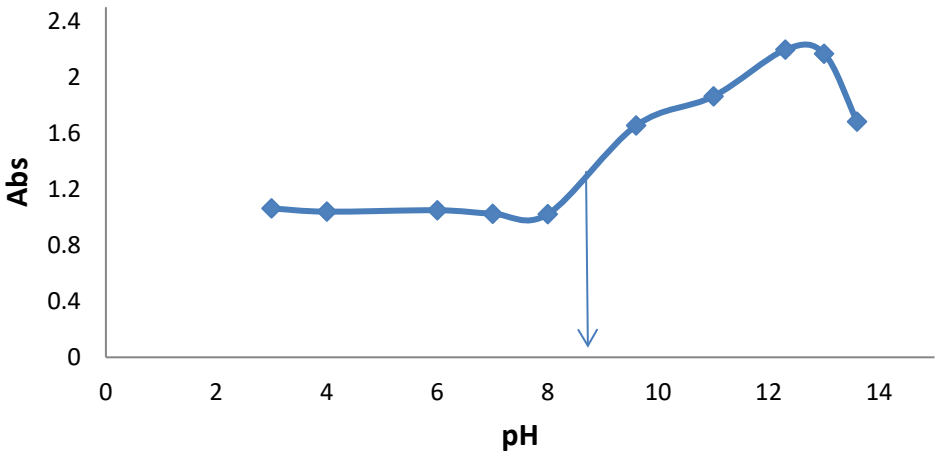

Figure 16. Absorbance–pH plot of 4-HAR at 445 nm

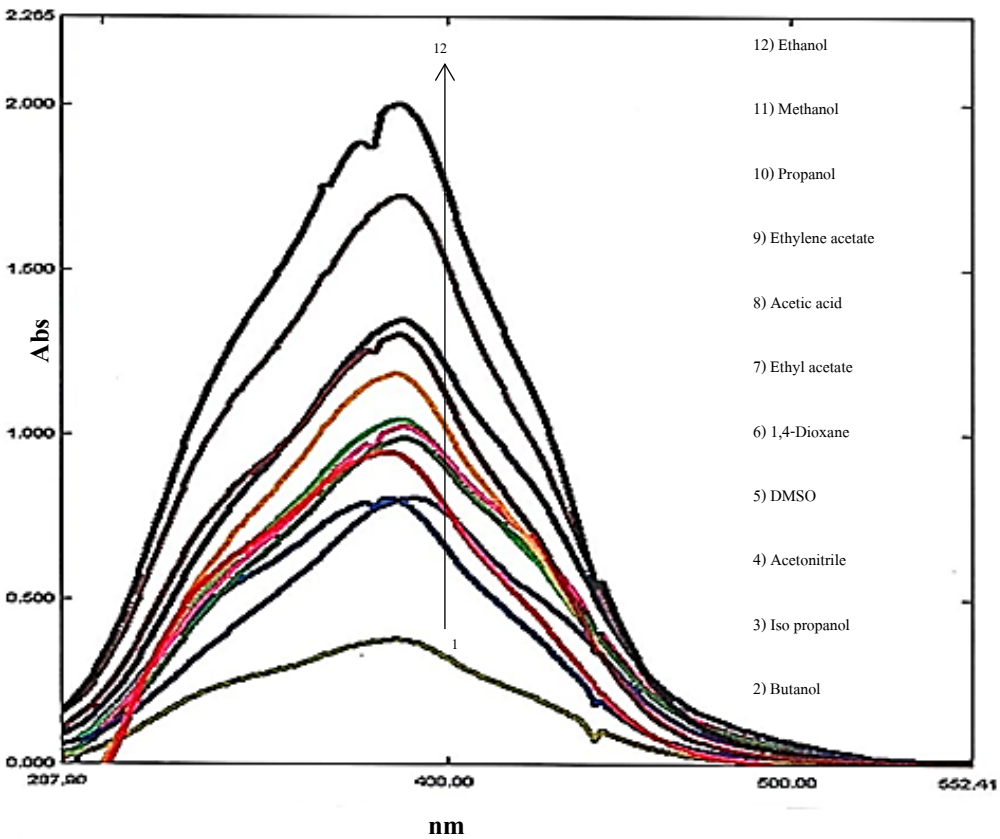

Figure 17. Spectra for 4-HAR measured in the referred solvents; solvents were arranged in the legend based on the increasing intensity of absorption at the point where the line is passed.

$$\nu = \nu o + s\pi^* + b\beta + a\alpha \quad (1)$$

Table 2 lists the eleventh solvents, which are divided into two groups A and B, as well as their parameters. It has been demonstrated that the azo compound absorption frequencies in different solvents have a suitable relationship with parameters of α, π^* and β. The degree of success of equation 1 is shown in Tables 3 and 4 from high values of correlation coefficient. Table 5 shows the results of the multiple regression analysis, and the *vo, s, b* and *a* coefficients have 95% confidence levels of significance [45, 46]. From the aforementioned conclusions, it is obvious that the reliance on a single solvent property to demonstrate the effects of a solute-solvent interaction is insufficient. This is shown in Figure 18 by the low correlation coefficient when the wavenumber was plotted against the solvent's dielectric constant.

Table 2. 4-HAR absorption maxima in various solvents and selective Kamlet-Taft solvent parameters (ε: dielectric constant)

Solvent	λmax	v, cm^{-1}	π	α	β	ε
Group A;						
Acetic acid	382	26178.01	0.64	1.12	0.45	6.2
n-Butanol	388	25773.13	0.47	0.84	0.84	18
Methanol	385	25974.02	0.6	0.93	0.63	32.6
n-Propanol	387	25839.79	0.52	0.84	0.9	20.3
1,4 Dioxan	386	25906.73	0.62	0.08	0.48	20.7
Ethanol	387	25839.79	0.54	0.83	0.75	24.6
Group B;						
Ethyl acetate	386	25906.73	0.45	0	0.45	6
Ethylene chloride	387	25839.79	0.82	0.4	0.43	10.4
DMSO	390	25641.02	0.52	0.6	0.48	4.81
Iso propanol	387	25839.79	0.72	0.64	0.5	13.4
Ether	386	25906.73	0.24	0	0.47	4.3

Table 3. Data of regression of linear solvation equation applied on the studied eleven solvents, group A

	Regression Statistics
Multiple R	0.979225
R Square	0.958881
Adjusted R Square	0.897203
Standard Error	46.26035
Observations	6

ANOVA

	df	*SS*	*MS*	*F*	*Significance*
Regression	3	99809.33	33269.78	15.54648	0.06104
Residual	2	4280.04	2140.02		
Total	5	104089.4			

	Coefficients	*Standard Error*	*t Stat*	*P-value*	*Lower 95%*	*Upper 95%*	*Lower 95.0%*	*Upper 95.0%*
Intercept	25299.34	678.2615	37.30027	0.000718	22381.02	28217.66	22381.02	28217.66
X Variable 1	1189.279	864.8076	1.375195	0.302852	-2531.69	4910.246	-2531.69	4910.246
X Variable 2	209.736	61.04569	3.435722	0.075275	-52.9224	472.3944	-52.9224	472.3944
X Variable 3	-318.371	310.0047	-1.02699	0.412402	-1652.21	1015.472	-1652.21	1015.472

Table 4. Data of regression of linear solvation equation applied on the studied eleven solvents, group B

	Regression Statistics
Multiple R	0.923371
R Square	0.852615
Adjusted R Square	0.410459
Standard Error	63.85126
Observations	5

ANOVA

	df	*SS*	*MS*	*F*	*Significance*
Regression	3	23585.11	7861.705	1.928314	0.476519
Residual	1	4076.984	4076.984		
Total	4	27662.1			

	Coefficients	*Standard Error*	*t Stat*	*P-value*	*Lower 95%*	*Upper 95%*	*Lower 95.0%*	*Upper 95.0%*
Intercept	24168.31	1029.239	23.48172	0.027095	11090.59	37246.04	11090.59	37246.04
X Variable 1	673.8866	301.295	2.236634	0.26766	-3154.43	4502.203	-3154.43	4502.203
X Variable 2	-547.967	245.3482	-2.23342	0.268001	-3665.41	2569.478	-3665.41	2569.478
X Variable 3	3063.508	2070.01	1.479948	0.378299	-23238.5	29365.48	-23238.5	29365.48

Table 5. Regression fits to equation 1 solvatochromic parameters

4-HAR	vo	s	b	a	R	F
In group A	25299.3	1189.23	209.74	-318.37	0.9589	15.5465
In group B	24168.3	673.89	-547.97	3063.51	0.8526	1.92831

R- Correlation coefficient; F- Fisher's test

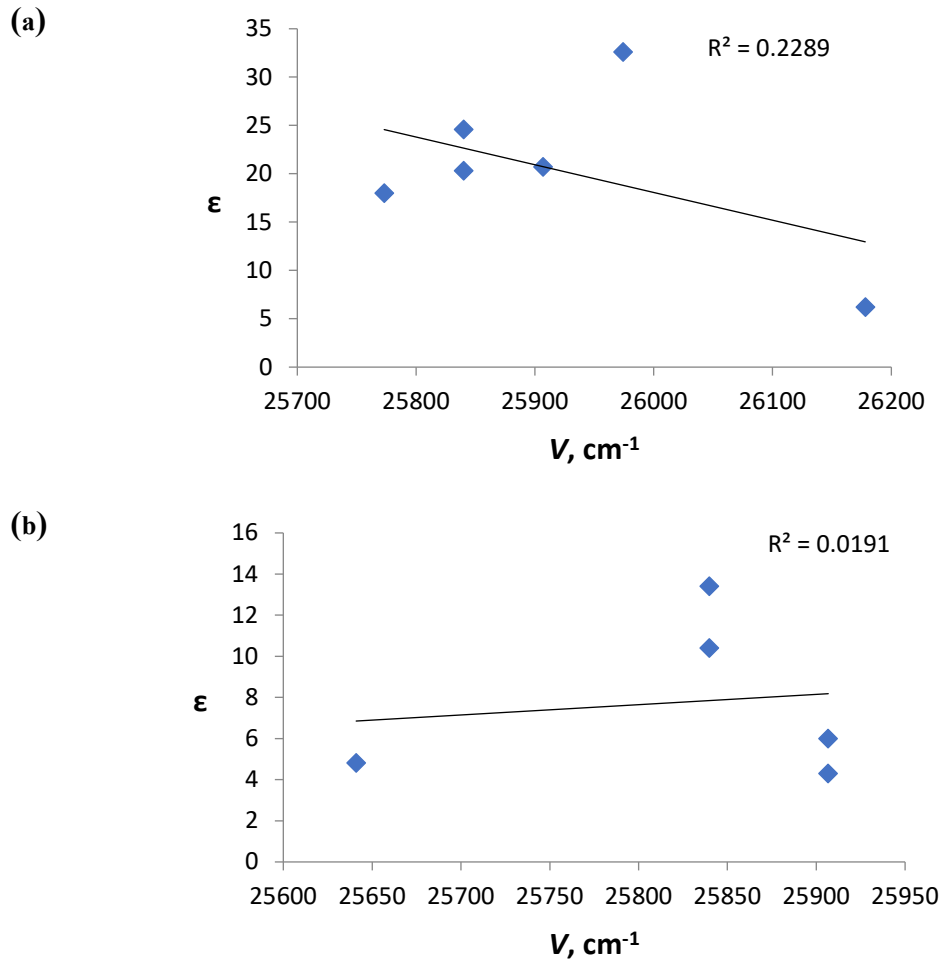

Figure 18. Variation of V, $cm^{-1}$of 4-HAR as a function of solvent dielectric constant (a) Group A solvents and (b) Group B solvents

3.6 Devoting 4-HAR in analytical approach

After choosing the best concentration of 4-HAR, which was 1×10^{-4}M, gave a smooth spectrum with satisfactory absorbance, aa shown in Figure 19. Preliminary experiments were performed to investigate the reaction of more than 20 metal ions of the periodic table with 4-HAR under definite conditions of concentration, pH, and temperature. 4-HAR was examined with the metal ions; Hg^{2+}, Zn^{2+}, Cd^{2+}, Al^{3+}, K^{+}, Fe^{3+}, La^{3+}, Mg^{2+}, Sn^{2+}, Na^{+}, Li^{+}, Mn^{2+}, Co^{2+}, Ni^{2+}, Ce^{4+}, Cr^{3+}, WO_4^{2-}, Ca^{2+}, Ag^{1+}, Bi^{2+}, Pt^{2+}, Pd^{2+}, $Fe^{2+}$and Cu^{2+} After mixing the reactants and based on the appearance of new color, there was no color change with the examined metal ions except in the case of copper (II) and iron(II), for which the reaction was positive. For iron(II), the product was of red color, while for copper (II), the color of the resulting complex was a deep green color. The green color of copper meant that a more desirable shift in favor of the analytical method from the wavelength of maximum absorption of the reagent from one side and with little overlap by iron from the other side. Therefore, copper (II) was chosen and the deep green product was scanned in the range of 200-800nm, and it showed a maximum absorbance at a wavelength of 603 nm. The deep green solution of the product was measured versus the blank solution prepared in the same way without copper (II). This reaction was developed as a spectroscopic approach to determine copper (II). The experimental conditions for the ion reaction were optimized with 4-HAR and the results are shown as optimum reagent volume (Figure 20), pH (Figure 21), time (Figure 22), and temperature (Figure 23). After that, a standard calibration curve was constructed using 4-HAR (Figure 24). The stoichiometry of the complex (ratio of metal to ligand, M:L) was estimated by two methods; the continuous variations and the mole ratio method (Figure 25, A and B). In addition, the analytical parameters were calculated and are presented in Table 6. The obtained results demonstrate that the analytical method is effective, precise, and accurate enough for the determination of low copper(II) concentrations.

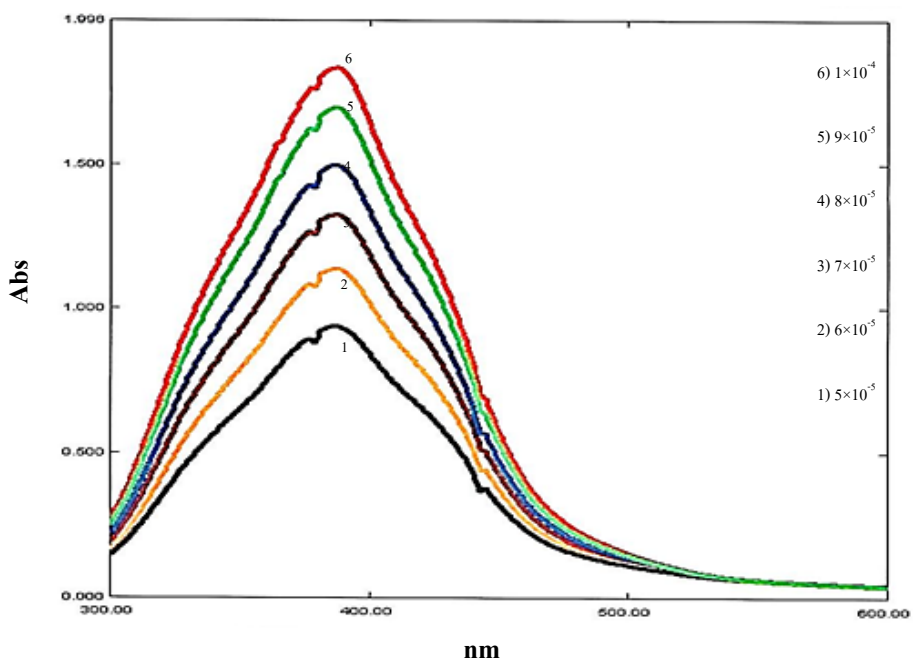

Figure 19. The best concentration(M) of 4-HAR

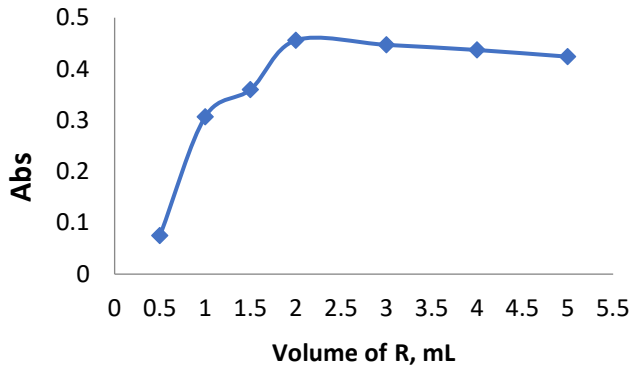

Figure 20. Effect of volume of reagent (1.0×10^{-4} M) on complex formation

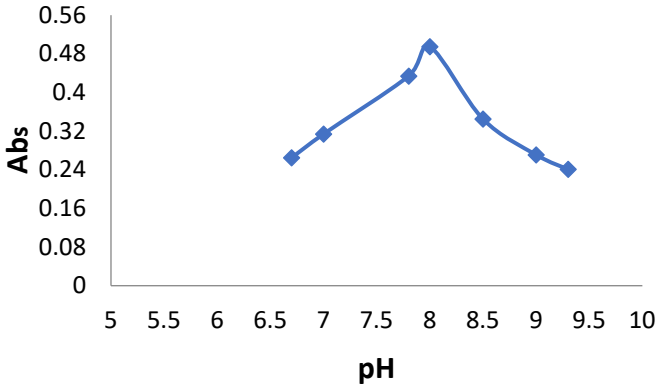

Figure 21. Effect of pH on complex formation

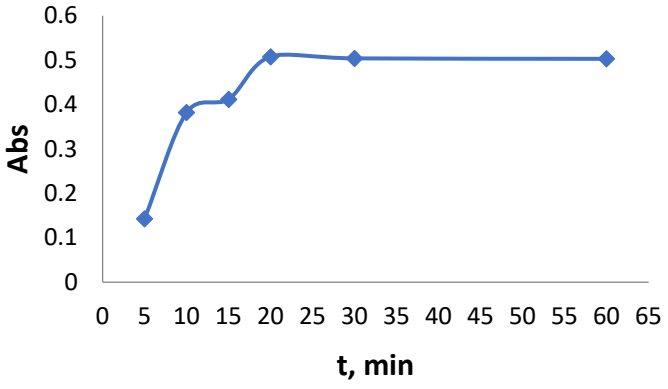

Figure 22. Stability of complex with time

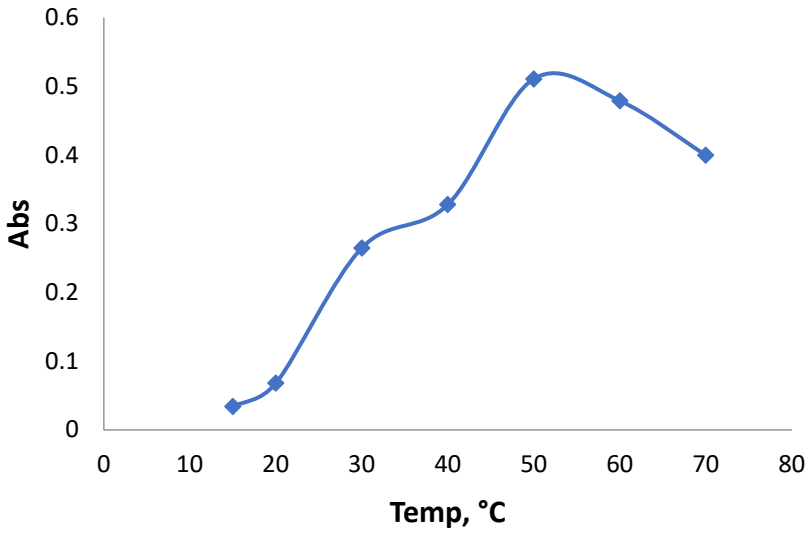

Figure 23. Effect of temperature on complex formation

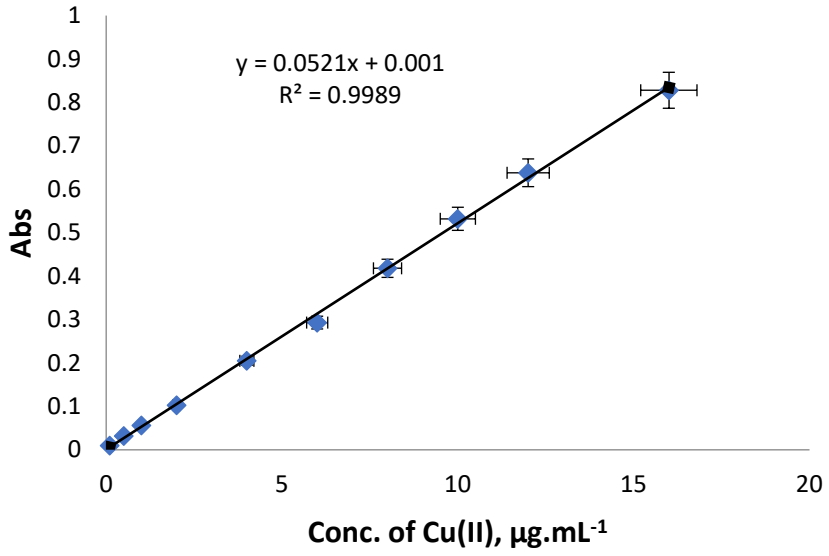

Figure 24. Calibration curve for copper(II) complex

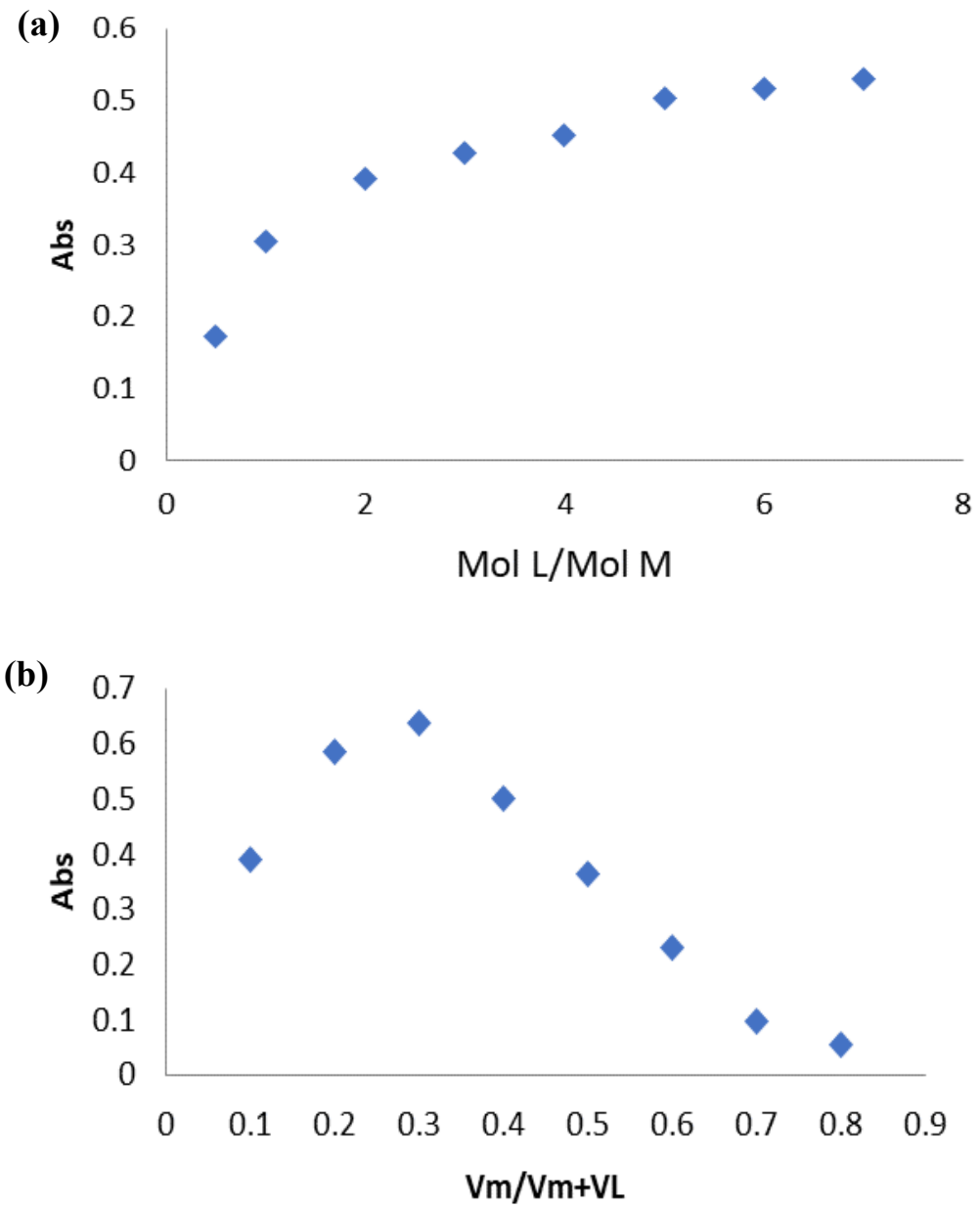

Figure 25. Methods of mole ratio (a) and continuous variation (b) for Cu(II) complex at pH=9

Table 6. Figures of merit for determination of copper(II) using 4-HAR

Analytical parameter	Value
Detection coefficient, R^2	0.9989
Correlation coefficient, r	0.9994
Linear Range, ($\mu g.mL^{-1}$)	0.30-16
Molar absorbance, ε ($L.mol^{-1}.cm^{-1}$)	3.314×10^3
Sandell's sensitivity, S ($\mu g.cm^{-2}$)	0.033
Standard deviation, S.D	0.0052
Detection limit, D.L ($\mu g.mL^{-1}$)	0.29
Quantitation limit, Q.L ($\mu g.mL^{-1}$)	0.99
Regression equation	Y = a + bx
Intercept (a)	0.001
Slope (b)	0.0521
$\%E_{rel}$	4.34, -3.94, -1.16
$\%R_{ec}$	104.34, 96.06, 98.39

* $\%E_{rel}$ and $\%R_{ec}$ were calculated for Cu(II) concentrations: 2.3, 3.8 and 6.8 $\mu g.mL^{-1}$

The method was used to find copper(II) in actual blood serum samples in order to judge the usefulness and validity of the method. Table 7 presents the outcomes. The findings indicated that recovery was nearly reached 100%. These findings also show that the common excipients did not seem to obstruct the identification of the desired ion. Additionally, the outcomes were contrasted with those of flame atomic absorption spectroscopy (FAAS). The concentration of copper(II) in each experiment was relatively close to the value predicted by the reference FAAS method.

Table 7. Determination of copper (II) in blood serum samples using the proposed method

Sample	Current study* µg.mL^{-1}	FAAS µg.mL^{-1}	%E_{rel}	%R_{ec}
#1	1.24±0.032 (0.041)	1.30	-4.62	95.38
#2	0.73±0.017(0.063)	0.75	-2.67	97.33
#3	0.51±0.022 (0.044)	0.54	-5.56	94.44
#4	1.16±0.031 (0.061)	1.20	-3.33	96.67
#5	0.75±0.033 (0.062)	0.79	-5.06	94.94
#6	1.54±0.024 (0.052)	1.51	1.99	101.99
#7	1.84±0.034 (0.038)	1.86	-1.08	98.92
#8	0.45±0.018 (0.042)	0.43	4.65	104.65
#9	0.94±0.025 (0.054)	0.92	2.17	102.17
#10	0.81±0.021 (0.036)	0.85	-4.71	95.29

*Mean of three independent analyses. Values of confidence limit (CL) calculated at 95% confidence level and two degrees of freedom (t=4.3)

4. Conclusions

The organic compound 4-(3-hydroxyphenylazo) resorcinol, 4-HAR, showed unique feature when reacting only with copper(II). The compound was characterized and it was found that there was agreement with the proposed structure. Among the important studies was the effect of the solvent and the successful application of the Kamlet-Taft linear solvation relationship. Further, the product of copper(II) with 4-HAR showed distinct green color. The formation of this color was utilized and applied for the determination of the presence of copper (II) in real samples of blood serum by a spectrophotometric method. Although the analyte in the studied samples was of a very low concentration that could not be estimated with reliable results using other spectrophotometric methods, it was determined by the current method with high sensitivity. Furthermore, the method proved to be inexpensively, less time consuming and well able to deliver high recoverability.

References

[1] Smith, D.G., Mitchell, L. and New, E.J., 2019. Pattern recognition of toxic metal ions using a single-probe thiocoumarin array. *Analyst*, 144(1), 230-236, DOI: 10.1039/c8an01747f.

[2] Sun, C., Shen, J., Cui, R., Yuan, F., Zhang, H. and Wu, X., 2019. Silver nanoflowers-enhanced Tb (III)/La (III) co-luminescence for the sensitive detection of dopamine. *Analytical and Bioanalytical Chemistry*, 411(7), 1375-138, DOI: 10.1007/s00216-018-01568-2.

[3] Park, M., Seo, S., Lee, S.J. and Jung, J.H., 2010. Functionalized Ni@ SiO_2 core/shell magnetic nanoparticles as a chemosensor and adsorbent for Cu^{2+} ion in drinking water and human blood. *Analyst*, 135(11), 2802-2805, DOI: 10.1039/C0AN00470G.

[4] Mathie, A., Sutton, G.L., Clarke, C.E. and Veale, E.L., 2006. Zinc and copper: pharmacological probes and endogenous modulators of neuronal excitability. *Journal of Pharmacology and Therapeutics*, 111(3), 567-583, DOI: 10.1016/j.pharmthera.2005.11.004.

[5] Zhang, W., Huang, D., Huang, M., Huang, J., Wang, D., Liu, X. and Meunier, B., 2018. Preparation of tetradentate copper chelators as potential anti-alzheimer agents. *ChemMedChem*, 13(7), 684-704, DOI: 10.1002/cmdc.201800184.

[6] Sparks, D.L. and Schreurs, B.G., 2003. Trace amounts of copper in water induce β-amyloid plaques and learning deficits in a rabbit model of alzheimer's disease. *Proceedings of the National Academy of Sciences*, 100(19), 11065-11069, DOI: 10.1073/pnas.1832769100.

[7] Sun, W., Han, Y., Li, Z., Ge, K. and Zhang, J., 2016. Bone-targeted mesoporous silica nanocarrier anchored by zoledronate for cancer bone metastasis. *Langmuir*, 32(36), 9237-9244, DOI: 10.1021/acs.langmuir.6b02228.

[8] Stern, B.R., 2010. Essentiality and toxicity in copper health risk assessment: overview, update and regulatory considerations. *Journal of Toxicology and Environmental Health*, *Part A*, 73(2-3), 114-127, DOI: 10.1080/15287390903337100.

[9] Bagherian, G., Arab Chamjangali, M., Shariati Evari, H. and Ashrafi, M., 2019. Determination of copper (II) by flame atomic absorption spectrometry after its perconcentration by a highly selective and environmentally friendly dispersive liquid–liquid microextraction technique. *Journal of Analytical Science and Technology*, 10(1), 1-11, DOI: 10.1186/s40543-019-0164-6.

[10] Pourreza, N. and Ghanemi, K., 2006. Determination of copper by flame atomic absorption spectrometry after solid-phase extraction. *Spectroscopy Letters*, 39(2), 127-134, DOI: 10.1080/00387010500531035.

[11] Chrastný, V. and Komárek, M., 2009. Copper determination using ICP-MS with hexapole collision cell. *Chemical Papers*, 63(5), 512-519, DOI: 10.2478/s11696-009-0057-z.

[12] Ornatsky, O., Kinach, R., Bandura, D., Lou, X., Tanner, S., Baranov, V., Nitz, M. and Winnik, M., 2008. Development of analytical methods for multiplex bio-assay with inductively coupled plasma mass spectrometry. *Journal of Analytical Atomic Spectrometry,* 23(4), 463-469, DOI: 10.1039/b710510j.

[13] Topcu, C., Lacin, G., Yilmaz, V., Coldur, F., Caglar, B., Cubuk, O. and Isildak, I., 2018. Electrochemical determination of copper (II) in water samples using a novel ion-selective electrode based on a graphite oxide–imprinted polymer composite. *Analytical Letters*, 51(12), 1890-1910, DOI: 10.1080/00032719.2017.1395035.

[14] Koga, T., Hirakawa, C., Sakata, Y., Noma, H., Nonaka, K. and Terasaki, N., 2017. Spectroscopic and electrochemical analysis of Cu (I) complex of copper sulfate electroplating solution and evaluation of plated films. *ECS Transactions*, 75(35), DOI: 10.1149/ma2016-02/20/1601.

[15] Zielenkiewicz, T., Zawadzki, J. and Radomski, A., 2012. XRF spectrometer calibration for copper determination in wood. *X-Ray Spectrometry*, 41(6), 371-373, DOI: 10.1002/xrs.2416.

[16] Chen, H., Jia, S., Zhang, J., Jang, M., Chen, X., Koh, K. and Wang, Z., 2015. Sensitive detection of copper(II) ions based on the conformational change of peptides by surface plasmon resonance spectroscopy. *Analytical Methods*, 7(20), 9237-9244, DOI: 10.1021/acs.langmuir.6b02228.

[17] Bayindir, S. and Toprak, M., 2019. A novel pyrene-based selective colorimetric and ratiometric turn-on sensing for copper. *Spectrochimica Acta Part A: Molecular and Biomolecular Spectroscopy*, 213, 6-11, DOI: 10.1016/j.saa.2019.01.053.

[18] Hashem, E.Y., Seleim, M.M. and El-Zohry, A.M., 2011. Environmental method for spectrophotometric determination of copper (II). *Green Chemistry Letters and Reviews*, 4(3), 241-248, DOI: 10.1080/17518253.2010.546370.

[19] Leelasattarathkul, T., Liawruangrath, S., Rayanakorn, M., Oungpipat, W. and Liawruangrath, B., 2006. The development of sequential injection analysis coupled with lab-on-valve for copper determination. *Talanta*, 70(3), 656-660, DOI: 10.1016/j.talanta.2006.03.047.

[20] Araújo, A.N., Costa, R.C. and Alonso-Chamarro, J., 1999. Colorimetric determination of copper in aqueous samples using a flow injection system with a pre-concentration poly (ethylenimine) column. *Talanta*, 50(2), 337-343, DOI: 10.1016/S0039-9140(99)00033-8.

[21] Naser, N., Taha, D. and Kahdim, K., 2012. Synthesis and characterization of an organic reagent 4-(6-bromo-2-benzothiazolylazo) pyrogallol and its analytical application. *Journal of Oleo Science*, 61(7), 387-392, DOI: 10.5650/jos.61.387.

[22] Pinto, J.J., Moreno, C. and García-Vargas, M., 2002. A simple and very sensitive spectrophotometric method for the direct determination of copper ions. *Analytical and Bioanalytical Chemistry*, 373(8), 844-848, DOI: 10.1007/s00216-002-1403-y.

[23] Purachat, B., Liawruangrath, S., Sooksamiti, P., Rattanaphani, S. and Buddhasukh, D., 2001. Univariate and simplex optimization for the flow-injection spectrophotometric determination of copper using nitroso-R salt as a complexing agent. *Analytical Sciences*, 17(3), 443-447, DOI: 10.2116/analsci.17.443.

[24] Rumori, P. and Cerdà, V., 2003. Reversed flow injection and sandwich sequential injection methods for the spectrophotometric determination of copper (II) with cuprizone. *Analytica Chimica Acta,* 486(2), 227-235, DOI: 10.1016/S0003-2670(03)00493-8.

[25] Thakur, M. And Deb, M.K., 1999. The use of 1-[pyridyl-(2)-azo]-naphthol-(2) in the presence of TX-100 and N, N′-diphenylbenzamidine for the spectrophotometric determination of copper in real samples. *Talanta*, 49(3), 561-569, DOI: 10.1016/S0039-9140(99)00054-5.

[26] Chaisuksant, R., Palkawong-na-ayuthaya, W. and Grudpan. K., 2000. Spectrophotometric determination of copper in alloys using naphthazarin *Talanta*, 53(3), 579-585, DOI: 10.1016/S0039-9140(00)00534-8.

[27] Admasu, D., Reddy, D.N. and Mekonnen, K.N., 2016. Spectrophotometric determination of Cu (II) in soil and vegetable samples collected from Abraha Atsbeha, Tigray, Ethiopia using heterocyclic thiosemicarbazone. *SpringerPlus*, 5(1), DOI: 10.1186/s40064-016-2848-3.

[28] Naser, A.N., Kasim, M. and Zainab, A.K., 2018. New approach for determination of sulfadiazine in pharmaceutical preparations using 4(4-sulphophenylazo)pyrogallol: Kinetic spectrophotometric method. *Spectrochimica Acta Part A: Molecular and Biomolecular Spectroscopy*, 201, 267-280, DOI: 10.1016/j.saa.2018.05.012.

[29] Winkler, W. and Arenhövel-Pacuła, A., 2000. The use of phenylfluorone in the presence of cetylpyridinium chloride and Triton X-100 for the spectrophotometric determination of copper (II) in blood serum. *Talanta*, 53(2), 277-283, DOI: 10.1016/S0039-9140(00)00406-9.

[30] Pavia, D., Lampman, G.M., Kriz, G.S. and Vyvyan, J.R., 2013. *Introduction to Spectroscopy*, 5th ed. Stamford: Cengage Learning.

[31] Ahmed, F., Dewani, R., Pervez, K., Mahboob, J. and Soomro, S., 2016. Non-destructive FT-IR analysis of mono azo dyes. *Bulgarian Chemical Communications*, 48, 71-77, DOI: 10.1515/rput-2017-0012.

[32] Raymond, A., Jonathan, B., Lee, G. and Manuel, P., 2006. 1H chemical shifts in NMR: Part 23, the effect of dimethyl sulphoxide versus chloroform solvent on 1H chemical shifts. *Magnetic Resonance in Chemistry*, 44, 491-509, DOI: 10.1002/mrc.1747.

[33] Kermit, K., Robert, K., Marcos, N., John, L., Liang, L. and Yasuhide, N., 2013. Definitions of terms relating to mass spectrometry (IUPAC Recommendations 2013). *Pure and Applied Chemistry*, 85, 1515-1609, DOI: 10.1351/PAC-REC-06-04-06.

[34] Nicolescu, T.O., 2017. Interpretation of Mass Spectra. In: M. Aliofkhazraei, ed. *Mass Spectrometry*. London: IntechOpen, pp. 24-78.

[35] Liudmil, A., 2019. Tautomerism in azo and azomethyne dyes: When and if theory meets experiment. *Molecules*, 24, 2252-2266, DOI: 10.3390/molecules24122252.

[36] Denevaa, V., Lyčkab, A., Hristovaa, S., Crochetc, A., Frommc, K. and Antonova, L., 2019. Tautomerism in azo dyes: Border cases of azo and hydrazo tautomers as possible NMR reference compounds. *Dyes and Pigments*, 165, 157-163, DOI: 10.1016/j.dyepig.2019.02.015.

[37] Ramesh, M., Maniraj, J. And Ramesh, S., 2022. Thermal properties of the grass/cane fiber-based hybrid composites. Natural fiber-reinforced composites: In: S. Krishnasamy, S.M.K. Thiagamani, C. Muthukumar, R. Nagarajan and S. Siengchin, eds. *Natural Fiber-Reinforces Composite: Thermal Properties and Applications*. Weinheim: Wiley-VCH, pp. 135-151.

[38] Tafu, N. and Jideani, V., 2021. Characterization of novel solid dispersions of *Moringa oleifera* leaf powder using thermo-analytical techniques. *Processes*, 9(12), DOI: 10.3390/pr9122230.

[39] Mutar, M. and Ali, H., 2021. Preparation, characterization and analytical studies of novel azo dyes and diazo dyes. *Journal of Physics: Conference Series*, 2063(1), DOI: 10.1088/1742-6596/2063/1/012023.

[40] Ammar, J.W., Khan, Z.A., Ghazi, M.N. and Naser, N.A., 2021. Synthesis of a new organic probe 4-(4 acetamidophenylazo) pyrogallol for spectrophotometric determination of Bi (III) and Al (III) in pharmaceutical samples. *Reviews in Analytical Chemistry*, 40(1), 108-126, DOI: 10.1515/revac-2021-0125.

[41] Zhou, H., Liu, Y., Lu, Y., Dong, P., Guo, B., Ding, W. and Dong, B., 2016. In-situ crack propagation monitoring in mortar embedded with cement-based piezoelectric ceramic sensors. *Journal of Construction and Building Materials*, 126, 361-368, DOI: 10.1016/j.conbuildmat.2016.09.050.

[42] El-ansary, A.L. and Ali, A.A., 1984. Spectrophotometric determination of ionization constants of some 8-hydroxyquinoline azo dyes. *Chimie*, 30, 145-150.

[43] Abu-Bakr, M.S., El-Shahawy, A.S. and Ahmed, S.M., 1993. Spectrophotometric study of acid-base equilibria of 4-(2-benzothiazolylazo) resorcinol and 4-(2-benzothiazolylazo) salicylic acid in water-organic solvent media. *Journal of Solution Chemistry*, 22(7), 663-675, DOI: 10.1007/BF00646785.

[44] Kamlet, M.J. and Taft, R.W., 1985. Linear solvation energy relationships. Local empirical rules-or fundamental laws of chemistry? A reply to the chemometricians. *Acta Chemica Scandinava* B*,* 39, 611-628, DOI: 10.3891/acta.chem.scand.39b-0611.

[45] Zatloukal, F., Achbergerová, E., Gergela, D., Rouchal, M., Dastychová, L., Prucková, Z. and Vícha, R.,2021. Supramolecular properties of amphiphilic adamantylated azo dyes. *Dyes and Pigments*, 192, DOI: 10.1016/j.dyepig.2021.109420.

[46] Najm, M.A.A., Abd-Alrassol, K.S., Qasim, Q.A., Hussein, H.H. and AL-Salman, H.N.K., 2022. Spectrophotometric determination of folic acid using 1, 10-phenanthroline materials with ninhydrin reagent. *Materials Today: Proceedings,* 61(3), 865-872, DOI: 10.1016/j.matpr.2021.09.453.